Miner Deposita (2012) 47:607–622
DOI 10.1007/s00126-012-0406-7

LETTER

Molybdenite Re–Os and muscovite $^{40}Ar/^{39}Ar$ dating of quartz vein-type W–Sn polymetallic deposits in Northern Guangdong, South China

Hua-Wen Qi · Rui-Zhong Hu · Xiao-Fei Wang · Wen-Jun Qu · Xian-Wu Bi · Jian-Tang Peng

Received: 31 January 2010 / Accepted: 25 January 2012 / Published online: 17 February 2012

Abstract Northern Guangdong is an important part of Nanling tungsten–tin metallogenic belt, South China. The tungsten mineralization in this area consists of mainly quartz–wolframite vein-type mineralization, with W–Sn polymetallic deposits mostly distributed at the outer contact zone between concealed Late Jurassic granitic stocks and Cambrian–Ordovician low-metamorphosed sandstones and shales. Molybdenite Re–Os and muscovite $^{40}Ar/^{39}Ar$ isotopic dating of three typical tungsten vein-type deposits (Yaoling, Meiziwo, and Jubankeng) in northern Guangdong, show that two episodes of Late Jurassic W–Sn polymetallic mineralization occurred in this area: an early episode during the Late Jurassic (158–159 Ma) represented by the Yaoling, Hongling, and Meiziwo tungsten deposits, and a younger event during the Early Cretaceous (138 Ma) represented by the Jubankeng deposit. Analysis of available radiometric ages of several W–Sn deposits in the Nanling region indicate that these deposits formed at several intervals during the Mesozoic at 90–100, 134–140, 144–162, and 210–235 Ma, and that large-scale W–Sn mineralization in this region occurred mainly between 150 and 160 Ma.

Editorial handling: F. Barra

H.-W. Qi (✉) · R.-Z. Hu · X.-F. Wang · X.-W. Bi · J.-T. Peng
State Key Laboratory of Ore Deposit Geochemistry,
Institute of Geochemistry, Chinese Academy of Sciences,
Guiyang 550002, China
e-mail: qihuawen@vip.gyig.ac.cn

X.-F. Wang
Graduate University of Chinese Academy of Sciences,
Beijing 100049, China

W.-J. Qu
National Research Center of Geoanalysis,
Beijing 100037, China

Keywords Tungsten–tin deposits · Re–Os molybdenite dating · $^{40}Ar/^{39}Ar$ muscovite dating · Northern Guangdong · China

Introduction

Northern Guangdong is one of the most important producing areas of tungsten–tin resources in Southern China. There are 12 large to medium-sized deposits and dozens of minor occurrences distributed in this region, which account for more than 95% of total proven reserves of tungsten (about 21.88 Mt WO_3), lead, zinc, copper, and silver, and 50% of tin and antimony in Northern Guangdong. Tungsten mineralization in these deposits is present mainly as quartz–wolframite veins (Yaoling, Shirenzhang, Meiziwo, and Jubankeng deposits), in a few altered granites (Hongling deposit) or in scheelite skarns (Yaoling deposit; Chen 1983; RGNTD 1985; Luo et al. 2006; Wang et al. 2006). The high concentration of W–Sn polymetallic deposits and the diverse styles of mineralization make Northern Guangdong an ideal place for the study of tungsten mineralization. Research on ore genesis and ore-forming processes of these tungsten deposits can provide guidelines for the exploration of tungsten mineralization in the Northern Guangdong area and by extension to the whole Nanling region, which also includes the Southern Jiangxi, Southern Hunan, and northeastern Guangxi areas.

The quartz–wolframite vein-type deposits account for more than half of the total tungsten reserves of South China and make up for more than 80% of the tungsten deposits and tungsten occurrences discovered in this area (Liu and Ma 1993). Several deposits of this type, i.e., Yaoling, Hongling, Shirenzhang, and Meiziwo in Northern Guangdong were systematically prospected during the 1960s using the “five-story building” model. This model summarized the vertical zonation and mineralogical compositions of these quartz–wolframite veins, and thus provided important guidelines for the exploration of these deposits in South China (Guangdong Metallurgical and Geological Team 932 1966, 1967, 1976; RGNTD 1985; Liu and Ma 1993). However, after decades of mining, tungsten resources are rapidly decreasing and more geological studies are needed in order to refine or develop new exploration models. Determination of the age of these ore deposits is not only a key issue to understand the possible genetic relationship between regional granites and the W–Sn mineralization, but also to determine regional metallogenetic epochs. Molybdenite Re–Os and mica $^{40}Ar/^{39}Ar$ dating methods have proven to be two powerful tools for the precise age determination of ore deposits (i.e., Suzuki et al. 1996; Reynolds et al. 1998; Selby and Creaser 2001, 2004; Creaser et al. 2002; Du et al. 2004; Fraser et al. 2008; Mao et al. 2009). Tungsten mineralization ages from northern Guangdong are scarce. Fu et al. (2008) reported molybdenite Re–Os isochron ages for the Shirenzhang and Shigushan deposits, whereas Wang et al. (2010) presented a molybdenite Re–Os isochron age for Hongling. All three molybdenite Re–Os isochron ages are ~160 Ma. Additionally, two muscovite $^{40}Ar/^{39}Ar$ plateau ages have been reported, one for the Meiziwo deposit (Zhai et al. 2010; 156.0±0.6 Ma) and the second for the Jubankeng deposit (Fu et al. 2009; 139.2±1.5 Ma). In this paper, we present new mineralization ages for three tungsten deposits located in Northern Guangdong (Yaoling, Meiziwo and Jubankeng). We also provide a compilation and a discussion of the available geochronologic data for tungsten deposits from the Nanling region.

Regional geological setting

Northern Guangdong is located in the South China Caledonian Fold Belt. Post Caledonian uplift and Hercynian–Indosinian depressions extend from Southern Hunan to Northern Guangdong (Fig. 1). Regional exposed strata consist of Paleozoic Cambrian, Ordovician, and Silurian low-metamorphosed clastic sedimentary rocks, Devonian coastal and neritic facies (sandstones, shales and carbonates), and Quaternary eluvium, diluvium and alluvium. Regional exposed igneous rocks include the southern part of the Zhuguangshan composite

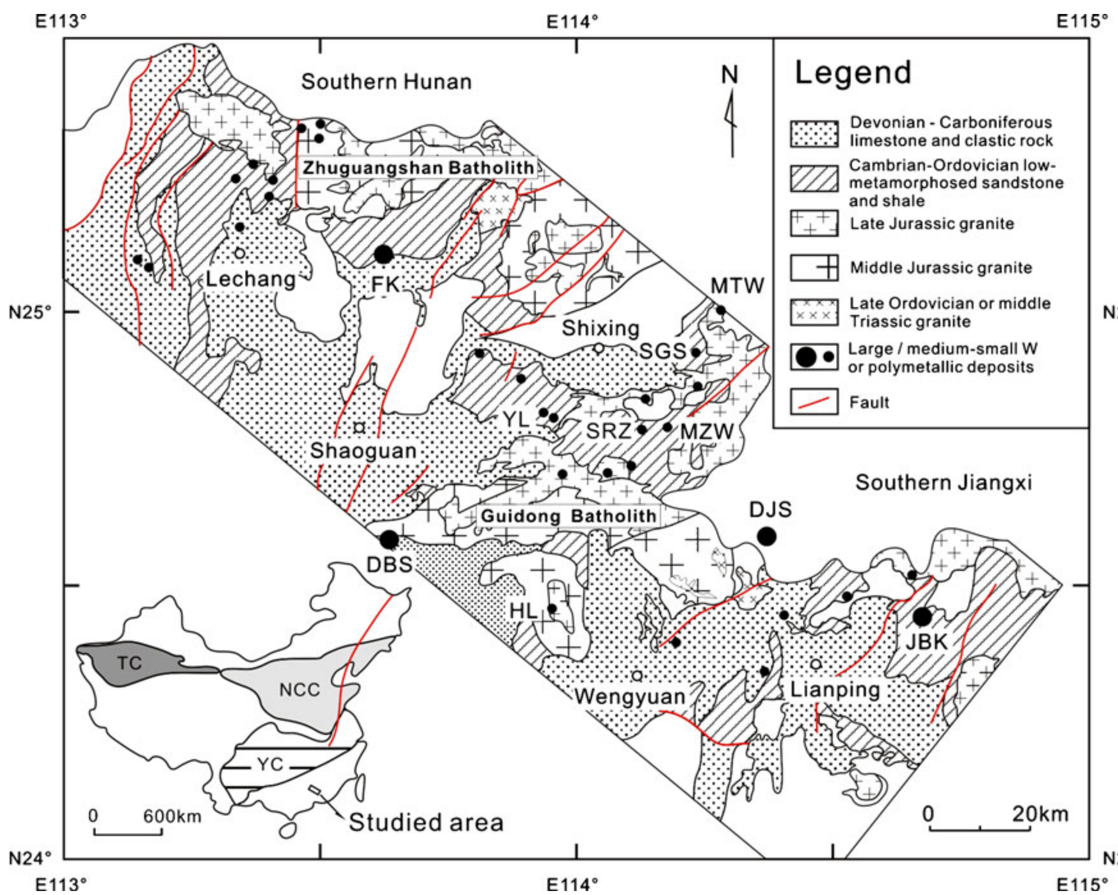

Fig. 1 Regional geological map of Northern Guangdong indicating the main mineral deposits in the area (after Luo et al. 2006). *YL* Yaoling, *SRZ* Shirenzhang, *MZW* Meiziwo, *HL* Hongling, *DJS* Dajishan, *JBK* Jubankeng, *SGS* Shigushan, *MTW* Miantuwo, *FK* Fankou Pb–Zn deposit, *DBS Dabaoshan polymetallic deposit, TC Tarim craton, NCC North China Craton, YC Yangtze Craton*

batholith, the Guidong composite batholith, as well as other small stocks. Tungsten mineralization is associated with Sn–Bi–(Mo)–Pb–Zn–(Ag) and it is very abundant in northern Guangdong with several deposits such as the super-large Jubankeng, the large Meiziwo, and other minor deposits (e.g., Yaoling, Shirenzhang, Hongling, Miantuwo) (Guangdong Metallurgical and Geological Team 932 1976; RGNTD 1985; Luo et al. 2006). Polymetallic Pb–Zn deposits (Fankou and Dabaoshan) are also present in the area (Fig. 1).

Geology of tungsten deposits

Yaoling

The Yaoling tungsten deposit is located in the southwestern limb of the Yaoling anticline complex (Fig. 2a). Exposed strata consist of Cambrian to middle Devonian low-grade metasedimentary quartzites, slates and interlayered siliceous conglomerates, cherts, siltstones, limestones, and argillaceous limestones. Late Jurassic granitoids outcrop extensively in the mining area. These granitoids are part of the Baijizhai granitic stock, Yaoling quartz porphyry dyke, and the concealed Yaoling granitic stock. The Yaoling anticline complex consists of mainly NE- or near SN trending subfolds. The Yaoling tungsten deposit comprises several ore blocks or areas (i.e., Beifeng'ao, Baolongli, Beifengwei, Xiaonandong, and Baijizhai; RGNTD 1985; Wang et al. 2006; Luo et al. 2006).

The Yaoling deposit involves three types of tungsten mineralization styles: quartz–wolframite vein-type mineralization, skarn-type, and altered granite-type scheelite mineralization. Forty-seven ore veins have been identified so far, which are mainly controlled by joint fractures (Fig. 2b). These veins crosscut the premineralization quartz porphyry dyke, and are displaced by postmineral faults (Fig. 2c). According to their orientation, these veins can be classified into three main groups: NW, NE, and NS; the NW group is the main tungsten-bearing vein set. The width of veins range from 0.15 to 0.38 m, and the average WO_3 grade is 1.35%. Wall rock alteration associated to quartz–wolframite veins includes silicification, chloritization, and sericitization, and the width of the alteration zone generally ranges from 0.2 to 2.2 m (Luo et al. 2006; Wang et al. 2006).

Skarn-type scheelite mineralization is mainly distributed in the southwestern Baijizhai segment. The ore bodies, commonly controlled by the contact zone and NE and NNW trending faults, occur at the contact zone between limestones, marls, and siltstones of the Middle Devonian Donggangling Group with the Baijizhai granitic stock (Fig. 2a). The scheelite orebody is more than 840 m wide, 200 m long, and 50 m thick, and mineralization is present in veinlets and disseminations within the skarn. WO_3 grades range from 0.006% to 0.97%, with an average grade of 0.43% (Wang et al. 2006).

Altered granite-type scheelite mineralization was found in the deep contact zone of the concealed Yaoling granite, where disseminated or star point-like scheelite aggregations occur along fractures or joint fractures. These fractures show tourmalinization and greisen-type alteration. The size of the orebody is more than 85 m long, and 0.68–1.30 m thick. WO_3 grades vary from 0.11% to 0.77%, with an average of 0.34% (Wang et al. 2006).

Meiziwo

The Meiziwo tungsten–tin deposit is a semiconcealed deposit within an area of 3.2 km^2 located in the northern part of the Guidong composite pluton, and at the eastern part of the Yaoling anticline complex. The tungsten-bearing quartz veins are controlled by a NW-trending fault system, and occur in strongly folded low-grade metasedimentary rocks (graywackes and slates) and Late Ordovician granodiorite (Fig. 2d). The NW-trending mineralized veins extend up to 2,550 m long and 1,250 m wide, vertically converging to the upper parts of the granodiorite (Fig. 2e). The quartz–wolframite veins show horizontal and vertical zonation. The northwestern sections of the veins have a higher concentration of WO_3 than the southeastern parts. Furthermore, mineralization in the upper sections of the veins are predominantly silicates and oxides with a small amount of cassiterite and locally high chalcopyrite zones, while sulfides and carbonates increase significantly in the deeper parts of the quartz–wolframite veins. The veins have an average grade of 1.1% WO_3, 0.05% Sn, and 0.06% Cu. The main ore minerals include wolframite, scheelite, cassiterite, arsenian pyrite, chalcopyrite, and molybdenite. Gangue minerals are mainly quartz, secondary feldspar, beryl, fluorite, tourmaline, and muscovite. Wall rock alteration is mainly greisenization and tourmalinization (Guangdong Metallurgical and Geological Team 932 1976).

Jubankeng

The Jubankeng tungsten deposit, located in the hinterland of the Jiulian Mountain, is not only a large quartz–wolframite vein-type deposit with polymetallic mineralization that shows the "five-story building" vertical zonation, but it is also the deposit with the largest tungsten reserves in China (RGNTD 1985). The deposit is located at the edge of the South China Caledonian Fold Belt, and at the northwest limb of the Jiulian anticline complex. Regional exposed units include Caledonian metamorphosed gray–green fine-grained quartz sandstones and interlayered slates and siltstones, NNW strike muldakaites, and NEE-trending lamprophyre dikes (Fig. 2f). Quartz–wolframite veins in this deposit can be divided into four groups according to strike:

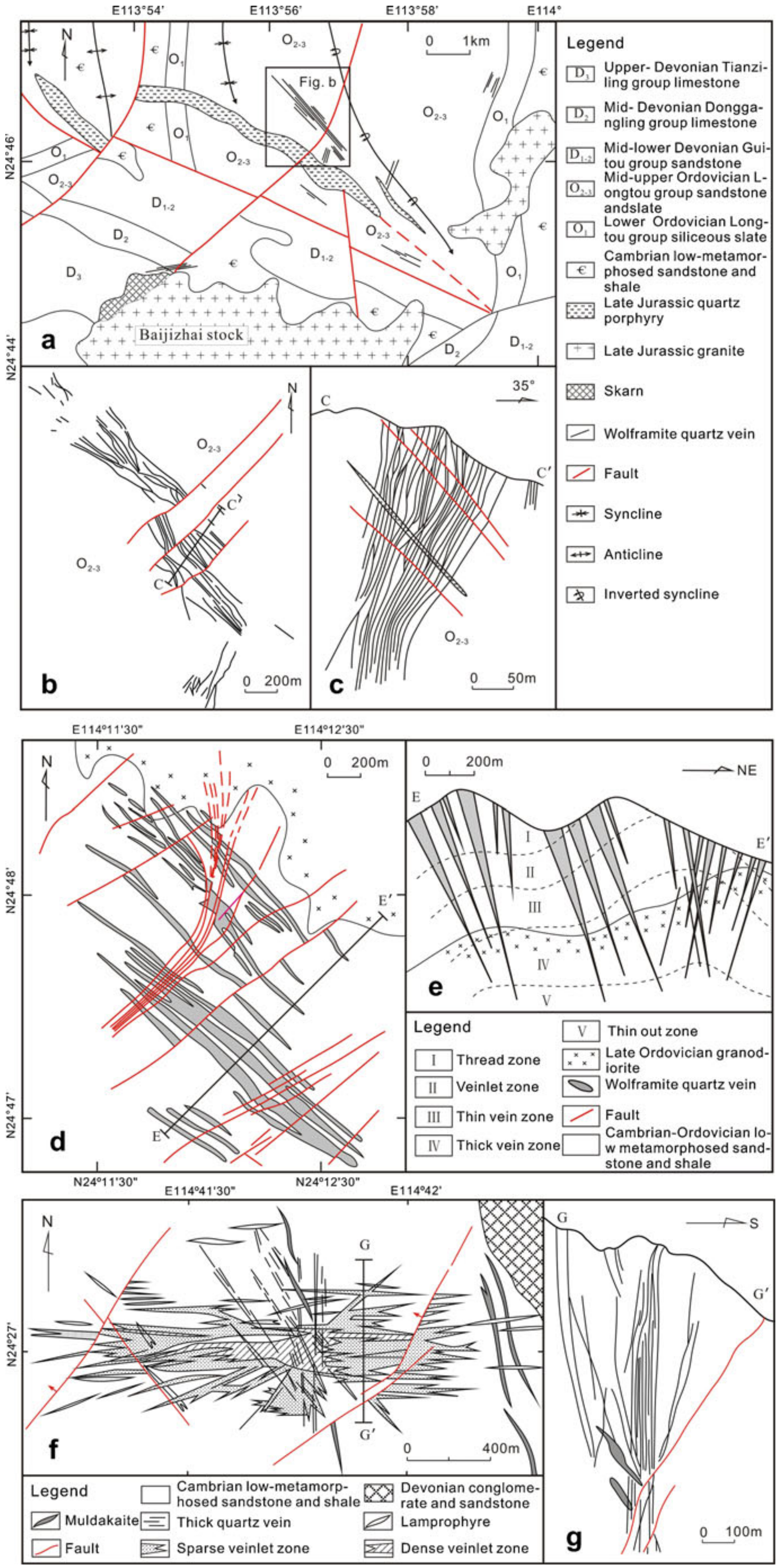

Fig. 2 Geologic maps and cross-sections of the Yaoling (**a**–**c**), Meiziwo (**d**, **e**), and Jubankeng (**f**, **g**) tungsten deposits, Northern Guangdong (after RGNTD 1985; Luo et al. 2006)

EW, NW, NE, and NS. Among these groups, the EW group is the largest, followed by the NEE, NNW, and NW groups; the NE and NWW trending vein sets are the smallest.

The EW vein group forms the main ore belt, stretching for more than 1,500 m with a width of 200–300 m (Fig. 2g). Quartz threads and wolframite-bearing quartz veinlets occur near the surface, whereas W–Sn and W–Sn–Zn–Cu quartz veins occur at both shallow and deeper parts of the deposit. The average grade is 0.35% WO_3, 0.125% Sn, 0.84% Zn, and 0.28% Cu. Nearly 30 different mineral species have been found in this deposit. The main paragenetic minerals include wolframite, cassiterite, chalcopyrite, sphalerite, galena, pyrite, molybdenite, quartz, protolithionite, trilithionite, topaz, chlorite, malachite, blue vitriol, and triplite. Ore textures include banded, miarolitic, massive, brecciated, and disseminated; the latter two are commonly found in sandstones and shales. The main types of hydrothermal alteration are silicification, topazization, tourmalinization, and chloritization (RGNTD 1985; Luo et al. 2006).

Sampling and analytical methods

Molybdenite-bearing quartz samples were systematically collected from quartz-wolframite veins #12 (MZ-25, MZ-26 and MZ-43), #18 (MZ-9 and MZ-42), and #57 (MZ-3 and MZ-7) at the 640–760 m level in the Meiziwo tungsten deposit, and from quartz-wolframite veins #26 (YL-3 and YL-11), #61 (YL-21), #62 (YL-16 and YL-23), #63 (YL-12 and YL-23), and #64 (YL-18) at the 479–532 m level in the Yaoling deposit. Most molybdenite aggregations are usually star point-like, blocky-shaped, distributed in the middle or edge of quartz–wolframite veins from Meiziwo, whereas some molybdenite samples from Yaoling are coarse and euhedral, with minor clay minerals (Fig. 3). Molybdenite samples were separated under a binocular microscope. After cleaning with water and drying, molybdenite separates (~0.8 to 1.3 g) were grounded to about 200 mesh. In order to avoid cross-contamination, all tools were cleaned with alcohol between samples preparation.

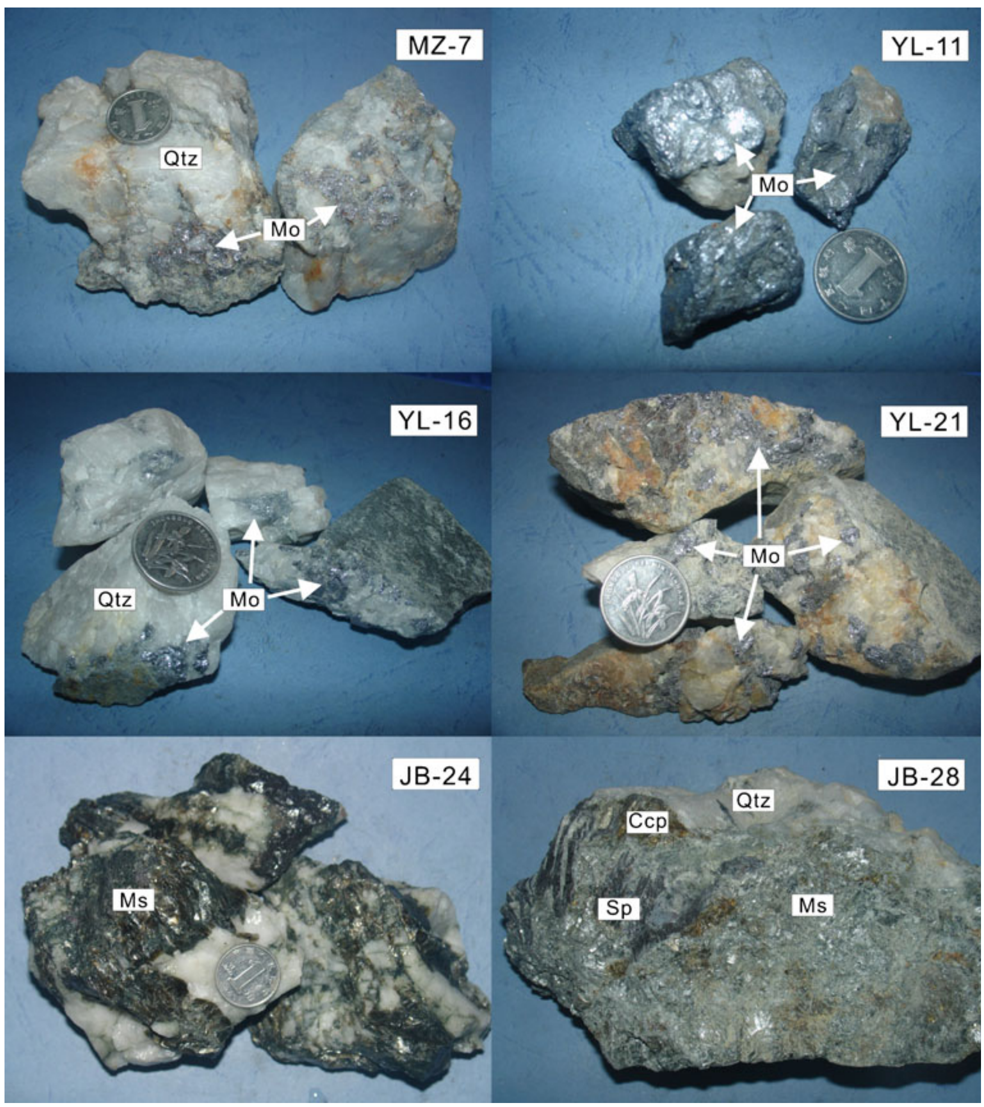

Fig. 3 Selected photographs of molybdenite and muscovite samples from Northern Guangdong. The diameter of the coin is 1.9 cm. Abbreviations of minerals: *Qtz* quartz, *Mo* molybdenite, *Ms* muscovite, *Ccp* chalcopyrite, *Sp* sphalerite

Re–Os isotope analyses were conducted at the National Research Center of Geoanalysis in Beijing, China, following the procedure of Du et al. (2004). Weighted samples (~0.3 g) were loaded into the bottom of Carius tubes (a thick-walled Pyrex glass ampoule) through long narrow neck funnels. Carius tubes were later submerged in a mixture of liquid nitrogen and alcohol at a temperature of −50°C to −80°C, then ^{185}Re and ^{190}Os spikes and HNO_3–HCl–H_2O_2 reagents were added. After the solutions within the Carius tubes were frozen, the tubes were sealed using a propane–oxygen torch and put into stainless steel jackets. The sample-solution mixture was heated in an oven to 200°C for 24 h to decompose the sample. After reaching room temperature, the Carius tube content was frozen again and the tube popped open. The solution was then transferred into a distillation flask with 40 ml MQ water. OsO_4 was separated from the solution by distillation at 105–110°C for 50 min and absorbed by a 10 ml MQ water trap. The residual solution was evaporated to dryness, and 10 ml 5 mol/l NaOH was added. After centrifugation, the supernatant was transferred into a 120 ml separatory funnel, in which Re was extracted by 10 ml acetone. The acetone phase was rinsed by 2 ml 5 mol/l NaOH and then evaporated to dryness in a Teflon beaker with 2 ml MQ water at 50°C. Several drops of concentrated HNO_3 and 30% H_2O_2 were added into the beaker. The solution was evaporated to dryness again to remove possible Os remnants. Residuals were dissolved with several ml of 2% HNO_3 for Re mass spectrometry measurements. If the salt content in the final Re-containing solution exceeded 1 mg/ml, the solution was further purified using cation exchange resin. Finally, Re and Os concentrations and isotopic ratios were determined using a TJA X-series inductively coupled plasma mass spectrometry. Re, Os and ^{187}Os blanks were 0.0038±0.0006, 0.0002, and 0.0001 ng, respectively, which are far less than the Re and Os contents in the analyzed molybdenite samples. Analytical results of molybdenite standard sample GBW04435 (HLP) measured using the same procedure yielded a mean age value of 220.9±3.3 Ma, within error to the certified value of 221.4± 5.6 Ma (Du et al. 2004).

Molybdenite is highly enriched in Re relative to Os, and hence almost all Os in molybdenite is radiogenic ^{187}Os (Luck and Allègre 1982; Suzuki et al. 1996). Therefore, a molybdenite Re–Os age can be calculated by using the ^{187}Re and ^{187}Os isotopic abundances. Re–Os isochron ages were calculated using ISOPLOT 3.70 program (see Ludwig 2004). The decay constant used in the age calculation was $\lambda^{187}\mathrm{Re}=1.666\times10^{-11}\ \mathrm{a}^{-1}$ (Smoliar et al. 1996).

Two muscovite separates were collected and separated from quartz–wolframite vein #440 (NNW striking; sample JB-24) and quartz–wolframite vein #350 (EW striking; sample JB-28) at the 380 m level in the Jubankeng tungsten deposit. Muscovite is generally associated with wolframite–quartz, chalcopyrite, and sphalerite (Fig. 3). The separates were washed repeatedly in an ultrasonic bath using deionized water and acetone. About 10 mg aliquots were wrapped in Al foil and stacked in quartz vials. After samples have been stacked, the sealed quartz vials were put in a quartz canister, which was wrapped with cadmium foil (0.5 mm in thickness) for shielding slow neutrons and for preventing interface reactions during irradiation. Samples were irradiated for 30 h in channel B4 of Beijing 49–2 reactor at the Chinese Academy of Nuclear-Energy Sciences. During irradiation, the vials were rotated at a speed of two cycles per minute to ensure uniformity of the irradiation. The muscovite standard Bern4M (18.74±0.20 Ma; Hall et al. 1984) was used to monitor the neutron flux.

^{40}Ar/^{39}Ar stepwise heating analyses were performed at the Argon Laboratory, Institute of Geology and Geophysics, Chinese Academy of Sciences, using a MM5400 mass spectrometer equipped with a Faraday cup and an ion counter (multiplier) for Ar isotopes measurement. The irradiated samples were loaded into a Christmas tree-type sample holder and degassed at 200–250°C for about 72 h in a high vacuum system. The samples were analyzed in 16 temperature steps from 780°C to total fusion at 1,480–1,500°C. Step-heating analysis was carried out in a double-vacuum resistance furnace. Samples were heated at each temperature step for 10 min and the extracted gasses were purified by two SAES Zr-Al getters (NP10). K_2SO_4 and CaF_2 crystals were analyzed to calculate Ca, *K* correction factors: $[^{36}\mathrm{Ar}/^{37}\mathrm{Ar}]_{\mathrm{Ca}}=2.609\times10^{-4}\pm1.418\times10^{-5}$, $[^{39}\mathrm{Ar}/^{37}\mathrm{Ar}]_{\mathrm{Ca}}=7.236\times10^{-4}\pm2.814\times10^{-5}$, $[^{40}\mathrm{Ar}/^{39}\mathrm{Ar}]_{\mathrm{K}}=2.648\times10^{-2}\pm2.254\times10^{-5}$. The decay constant value used in the age calculation was $\lambda=5.543\times10^{-10}\ \mathrm{a}^{-1}$ (Steiger and Jäger 1977). The data-processing software used was the ArArCALC 2.4 software (Koppers 2002). The plateau criteria involves: (1) at least 60% of the ^{39}Ar released in three or more contiguous steps, and the ages of these steps have to be concordant within 1 sigma error; (2) no resolvable slope on plateau; (3) no outliers or trends at upper or lower steps; and (4) probability of fit of plateau is >0.01.

Results

Re–Os molybdenite ages

Calculated ages for six molybdenite samples from the Meiziwo tungsten deposit range from 157.1±2.5 to 160.2±3.7 Ma. Sample MZ-7 yielded an age of 165.6±2.6 Ma, which we consider as an outlier (Table 1). The six samples yielded a weighted average age of 158.0±2.1 Ma (Fig. 4a), and an ^{187}Re–^{187}Os isochron age of 157.7±2.8 Ma with an initial ^{187}Os of 0.007±0.044 (ng/g; MSWD=0.35; Fig. 4b). This isochron age is basically the same as the reported muscovite

Table 1 Re and Os isotopic data for molybdenite samples from Meiziwo and Yaoling tungsten deposits, Northern Guangdong

Sample no.	Weight (g)	Re (ng/g)	Common Os (ng/g)	^{187}Re (ng/g)	^{187}Os (ng/g)	^{187}Re/^{188}Os	^{187}Os/^{188}Os	Age (Ma)
Meiziwo tungsten deposit								
MZ-3	0.30028	2,084±22	0.0002±0.0005	1,310±14	3.432±0.028			157.1±2.5
MZ-7	0.30058	1,377±13	0.0002±0.0014	865.2±8.1	2.390±0.023			165.6±2.6
MZ-9	0.30032	4,663±66	0.0002±0.0005	2,931±41	7.634±0.064			156.2±2.9
MZ-25	0.30001	722.1±7.4	0.0003±0.0006	453.8±4.6	1.201±0.010			158.6±2.4
MZ-26	0.30003	2,652±21	0.0002±0.0011	1,667±13	4.417±0.035			158.9±2.2
MZ-42	0.30031	4,044±36	0.0002±0.0006	2,542±23	6.684±0.067			157.6±2.5
MZ-43	0.30022	4,344±83	0.0002±0.0005	2,730±52	7.297±0.074			160.2±3.7
Yaoling tungsten deposit								
YL-3	0.29928	2,070±23	0.2004±0.0033	1,301±15	3.405±0.029	49,878±996	130.6±2.0	156.9±2.5
YL-3[a]	0.20054	2,105±17	0.2077±0.0034	1,323±11	3.425±0.031	48,959±903	126.7±2.0	155.1±2.3
YL-11	0.2999	460.0±4.6	0.0095±0.0010	289.1±2.9	0.754±0.006	234,485±23,757	611.1±61.5	156.2±2.4
YL-12	0.3003	3,826±53	0.3684±0.0040	2,404±33	6.345±0.051	50,151±882	132.3±1.2	158.2±2.8
YL-12[b]	0.30039	6,220±46	0.6050±0.0048	3,910±29	10.51±0.090	49,666±535	133.5±0.7	161.1±2.2
YL-16	0.30074	650.6±6.5	0.0225±0.0010	408.9±4.1	1.132±0.009	139,613±6,343	386.5±17.0	165.9±2.5
YL-16[a]	0.06066	689.5±7.1	0.0223±0.0018	433.4±4.4	1.068±0.012	149,017±12,372	367.1±30.3	147.7±2.6
YL-18	0.30021	458.6±4.4	0.0860±0.0018	288.3±2.7	0.773±0.008	25,762±582	69.08±1.44	160.7±2.6
YL-18[b]	0.30031	2,904±26	0.5403±0.0041	1,825±16	4.925±0.042	25,961±304	70.0±0.3	161.7±2.4
YL-21	0.30068	804.3±7.2	0.0593±0.0007	505.5±4.5	1.647±0.013	65,545±961	213.5±2.1	195.2±2.8
YL-21[a]	0.30048	804±6	0.0594±0.0012	505.3±3.8	1.597±0.014	65,326±1,433	206.4±4.1	189.3±2.7
YL-21[b]	0.30061	1,550±13	0.0573±0.0023	974.3±8.2	2.592±0.022	130,688±5,400	347.6±13.9	159.4±2.3
YL-23	0.30026	1,018±10	0.1878±0.0025	639.9±6.3	1.760±0.015	48,959±903	126.7±2.0	164.8±2.5
YL-23[b]	0.30051	3,531±34	0.1244±0.0012	2,219±21	5.927±0.047	137,044±1,855	366±2.6	160.1±2.4
YL-24	0.30059	1,128±10	0.0331±0.0008	709.2±6.0	1.871±0.017	164,791±4,191	434.8±10.2	158.2±2.3

All errors are reported at 2 sigma level

Common Os contents were calculated based on the Os isotopic abundance of Nier (1937) and measured ^{192}Os/^{190}Os ratios, ^{187}Os stands for total amount of isotope ^{187}Os

The uncertainty in Re and Os contents considers all sources of error, which include weighing error of samples and reagents, spikes calibration errors, mass fractionation correction errors, and measurement error of isotope ratios of analyzed sample, at the 95% confidence level

Molybdenite ages were calculated using ^{187}Re and ^{187}Os contents and the following equation: $T=1/\lambda\ [\ln (1+{}^{187}\mathrm{Os}/{}^{187}\mathrm{Re})]$, λ (^{187}Re decay constant)$=1.666\times10^{-11}\ a^{-1}$ (Smoliar et al. 1996). The uncertainty in these ages includes uncertainty in the Re decay constant (1.02%), at the 95% confidence level

Analytical data of aliquots in Italic format was excluded from age calculations

[a] Repeated analysis of the same aliquot

[b] Analysis of reselected aliquots

^{40}Ar/^{39}Ar plateau age of 155.97±0.59 Ma (Zhai et al. 2010) for this deposit.

The Re–Os isotopic compositions of eight molybdenite samples and their duplicates from the Yaoling tungsten deposit are listed in Table 1. Most of these samples (the same aliquots or reselected aliquots) were analyzed twice for two reasons: (1) these samples contain common Os (0.0095–0.6050 ng/g). High concentration of common Os (>0.1 ng/g) in molybdenite samples have been reported in some Cu–Fe–Au skarn deposits and in porphyry Cu–Mo deposits (Lu et al. 2006; Li et al. 2007; Wang et al. 2008a, b; Xie et al. 2009); and (2) while most calculated ages for the Yaoling samples range from 155.1±2.5 to 161.7±2.4 Ma, two samples (YL-16 and YL-21) show much younger (147.7±2.6 Ma) and older (up to 195.2±2.8 Ma) ages, respectively.

Our data shows that reproducibility of analytical data was significantly improved (Table 1) by increasing the amount of sample for molybdenite separation. Several grams were sufficient for samples with molybdenite clumps, while 2–3 kg of sample with disseminated star point-like molybdenite were needed in order to obtain a more homogeneous molybdenite separate and hence more accurate ages. For example, the calculated ages of reselected aliquots of YL-21[b] and YL-23[b] are 159.4±2.3 and 160.1±2.4 Ma, respectively. This also indicates that poor reproducibility of the former analysis of sample

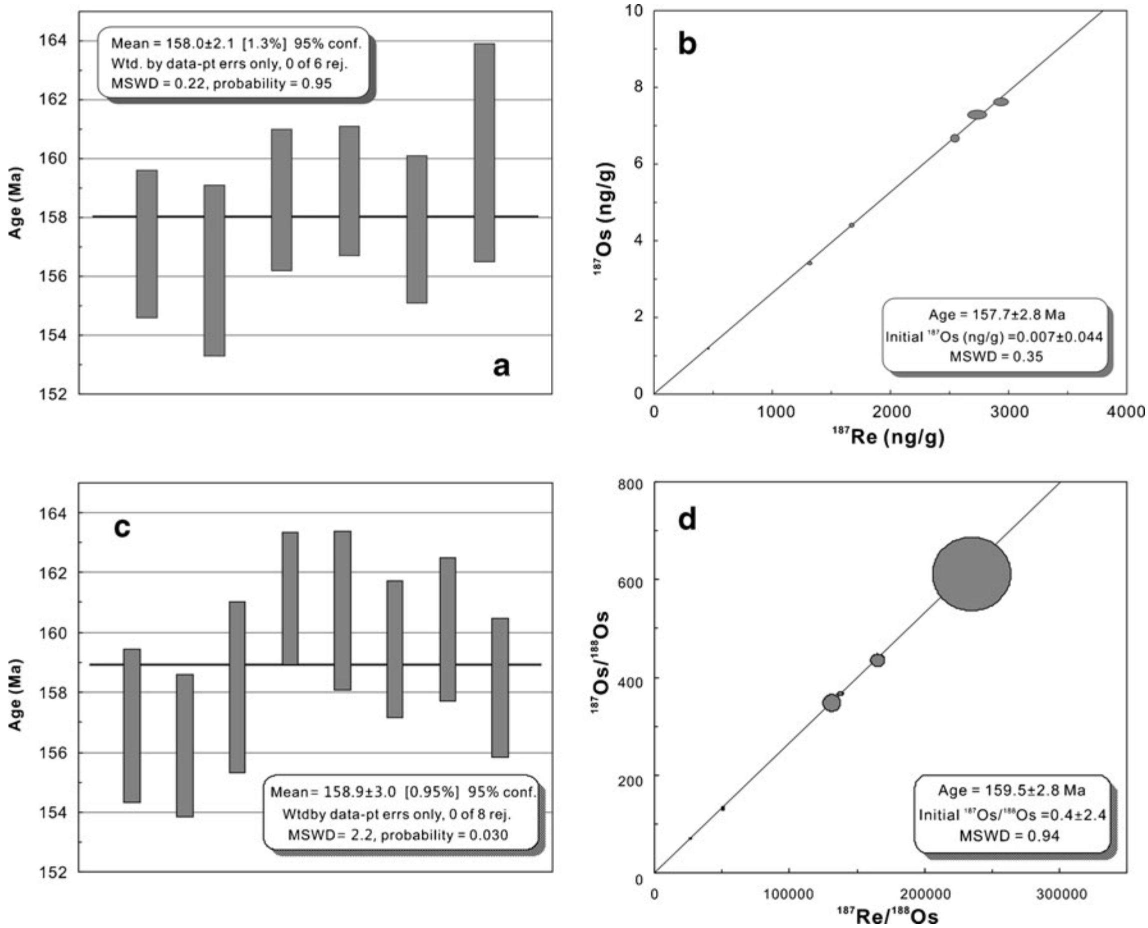

Fig. 4 Weighted average ages and Re–Os isochrons for molybdenite samples from the Meiziwo tungsten deposit (**a**, **b**) and Yaolingtungsten deposit (**c**, **d**)

YL-21 and YL-16 might have been caused by Re and ^{187}Os decoupling (Stein et al. 2003; Selby and Creaser 2004; Du et al. 2007; Takahashi et al. 2007). Moreover, the analysis of an aliquot of sample YL-18^{b} yielded a higher calculated initial ^{187}Os/^{188}Os ratio (up to 1.2±1.4). Therefore, the sample aliquots that yielded scattered erroneous ages (YL-16, YL-21, YL-23, YL-3, and YL-18^{b}) were excluded from the weighted average and isochron age calculation (Table 1). Eight analytical results define a weighted average age of 158.9±3.0 Ma (Fig. 4c), and ^{187}Re/^{188}Os–^{187}Os/^{188}Os isochron age of 159.5±2.8 Ma with an initial ^{187}Os/^{188}Os ratio of 0.4±2.4 (MSWD=0.94; Fig. 4d). These aliquots also yielded an ^{187}Re–^{187}Os isochron age of 160.3±2.0 Ma with an initial ^{187}Os (ng/g) of −0.020±0.042 (MSWD=3.2).

^{40}Ar/^{39}Ar isotopic data for muscovite samples from the Jubankeng deposit

^{40}Ar/^{39}Ar analytical results are shown in Table 2. Figure 5 shows the step-heating age spectra and inverse isochrons for samples JB-24 and JB-28. The age spectra of JB-24 shows a flat plateau with more than 95% of $^{39}Ar_K$ released, indicating that K and radiogenic ^{40}Ar* in the samples are distributed homogeneously and K–Ar isotopic systematics remained closed from heating disturbance during the geological history of the sample. Twelve continuous steps (900–1,180°C) of one muscovite sample (JB-24) yielded a well-defined weighted plateau age of 138.1±1.5 Ma, and a ^{39}Ar/^{40}Ar-^{36}Ar/^{40}Ar inverse isochron with an age of 138.0±1.7 Ma and an initial ^{40}Ar/^{36}Ar ratio of 297.0±17.6 (MSWD=5.53; Fig. 5a, b). The age spectra of JB-28 show some variations and cannot be considered a plateau. However, five continuous steps (1,100–1,280°C) of this muscovite sample with 29.41% of total ^{39}Ar yielded a weighted average age of 137.9±1.4 Ma and an ^{39}Ar/^{40}Ar-^{36}Ar/^{40}Ar inverse isochron age of 137.8±3.3 Ma with an initial ^{40}Ar/^{36}Ar ratio of 301.0±91.5 (MSWD=0.24; Fig. 5c, d). The initial ^{40}Ar/^{36}Ar ratios of these isochrons are consistent with that of air (295.5±0.5, Nier 1950; 298.56±0.31, Lee et al. 2006) within uncertainty, indicating that there is no excess argon in these samples. These ^{40}Ar/^{39}Ar ages are consistent with the ^{40}Ar/^{39}Ar plateau age of 139.2±1.5 Ma reported by Fu et al. (2009).

Table 2 $^{40}Ar/^{39}Ar$ analytical data for two muscovite samples from the Jubankeng tungsten deposit, South China

Temp. (°C)	$^{40}Ar/^{39}Ar$	$^{37}Ar/^{39}Ar$	$^{36}Ar/^{39}Ar$	$^{40}Ar^{*}/^{39}Ark$	$^{40}Ar^{*}$ (%)	^{39}Ark (%)	Age (Ma)
JB-24, sample weight=11.1 mg, J=0.0047870±0.0000239							
780°C	477.79099	0.04305	1.53106	25.368346	5.31	0.43	207.3±88.0
860°C	217.2321	0.01063	0.62488	32.58407	15.00	2.79	262.1±36.0
900°C	31.75755	0.00548	0.05138	16.574733	52.19	8.64	138.1±3.1
930°C	18.22043	0.00403	0.00575	16.520917	90.67	13.70	137.6±1.0
960°C	17.56433	0.00208	0.00322	16.612027	94.58	13.64	138.4±1.0
990°C	17.76482	0.01377	0.00415	16.538904	93.10	10.58	137.8±0.9
1,020°C	17.93824	0.00707	0.0051	16.431315	91.60	10.05	136.9±1.0
1,050°C	17.78648	0.00616	0.00492	16.332085	91.82	9.49	136.1±1.0
1,080°C	18.04924	0.00659	0.00525	16.496981	91.40	7.30	137.4±1.1
1,110°C	17.87563	0.00569	0.00423	16.624454	93.00	14.94	138.5±0.9
1,140°C	17.83626	0.02619	0.0037	16.744841	93.88	6.52	139.4±0.9
1,180°C	18.41341	0.09762	0.00537	16.835842	91.42	0.92	140.2±1.7
1,260°C	19.3439	0.07692	0.00822	16.921105	87.47	0.61	140.8±1.4
1,340°C	27.3628	0.60769	0.03636	16.674163	60.91	0.09	138.9±4.6
1,480°C	21.99897	0.1637	0.01443	17.749303	80.67	0.29	147.5±2.2
JB-28, sample weight=8.55 mg, J=0.0048160±0.0000241							
780°C	216.8999	0.13721	0.70233	9.371856	4.32	0.10	79.8±47.6
860°C	382.10652	0.00183	1.21447	23.23039	6.08	1.45	191.8±72.2
910°C	57.80553	0.00172	0.14627	14.582482	25.23	5.19	122.7±8.8
950°C	19.61653	0.00221	0.01155	16.20486	82.61	11.4	135.9±1.3
980°C	17.59472	0.00332	0.00482	16.17147	91.91	10.41	135.6±1.3
1,000°C	17.23775	0.00244	0.00432	15.961731	92.6	8.19	133.9±1.0
1,020°C	17.09121	0.00145	0.00442	15.784811	92.36	8.64	132.5±1.3
1,050°C	17.33215	0.00128	0.00519	15.799412	91.16	10.63	132.6±1.0
1,080°C	17.6631	0.00041	0.00492	16.208418	91.76	13.54	135.9±1.1
1,110°C	17.63433	0.00022	0.00392	16.47535	93.43	21.44	138.1±1.2
1,140°C	17.50443	0.00829	0.00361	16.438389	93.91	4.04	137.8±1.1
1,180°C	17.43735	0.01542	0.00341	16.432053	94.23	1.82	137.7±1.1
1,230°C	17.64004	0.01395	0.00379	16.520504	93.65	1.28	138.4±1.5
1,280°C	18.13526	0.00434	0.00569	16.453541	90.73	0.83	137.9±1.4
1,400°C	21.88677	0.21013	0.01596	17.190415	78.53	0.24	143.8±2.6
1,500°C	18.18078	0.02312	0.00457	16.833337	92.59	0.79	141.0±1.8

All errors are reported at 2 sigma level

Discussion

Mineralization ages of W polymetallic deposits in Northern Guangdong

Molybdenite samples from the Meiziwo tungsten deposit yielded a weighted average age of 158.0±2.1 Ma and $^{187}Re–^{187}Os$ isochron age of 157.7±2.8 Ma. Both ages are identical within error and represent the mineralization age of this deposit. Molybdenites from the Yaoling deposit contain common Os, which is about 300 times higher than average common Os concentration observed in other molybdenites (~0.0002 ng/g). However, the Re–Os age determined using the $^{187}Re–^{187}Os$ concentration plot (160.3±2.0 Ma) and the traditional $^{187}Re/^{188}Os–^{187}Os/^{188}Os$ plot (159.5±2.8 Ma) are within error, and they are also within error of the weighted average age (158.9±3.0 Ma) determined from the individual Re–Os model ages for the Yaoling samples (Table 1).

The Re–Os ages for Meiziwo (157.7±2.8 Ma) and for Yaoling (159.5±2.8 Ma) coupled with previously reported Re–Os molybdenite isochron ages of 159.1±2.2, 154.2±2.7, and 159.1±3.0 Ma for the Shirenzhang W deposit, Shigushan W-Bi deposit and Hongling W deposit, respectively (Fu et al. 2007; Wang et al. 2010), overlap with each other within uncertainties, and hence we interpret them as representing an early episode of tungsten mineralization in Northern Guangdong.

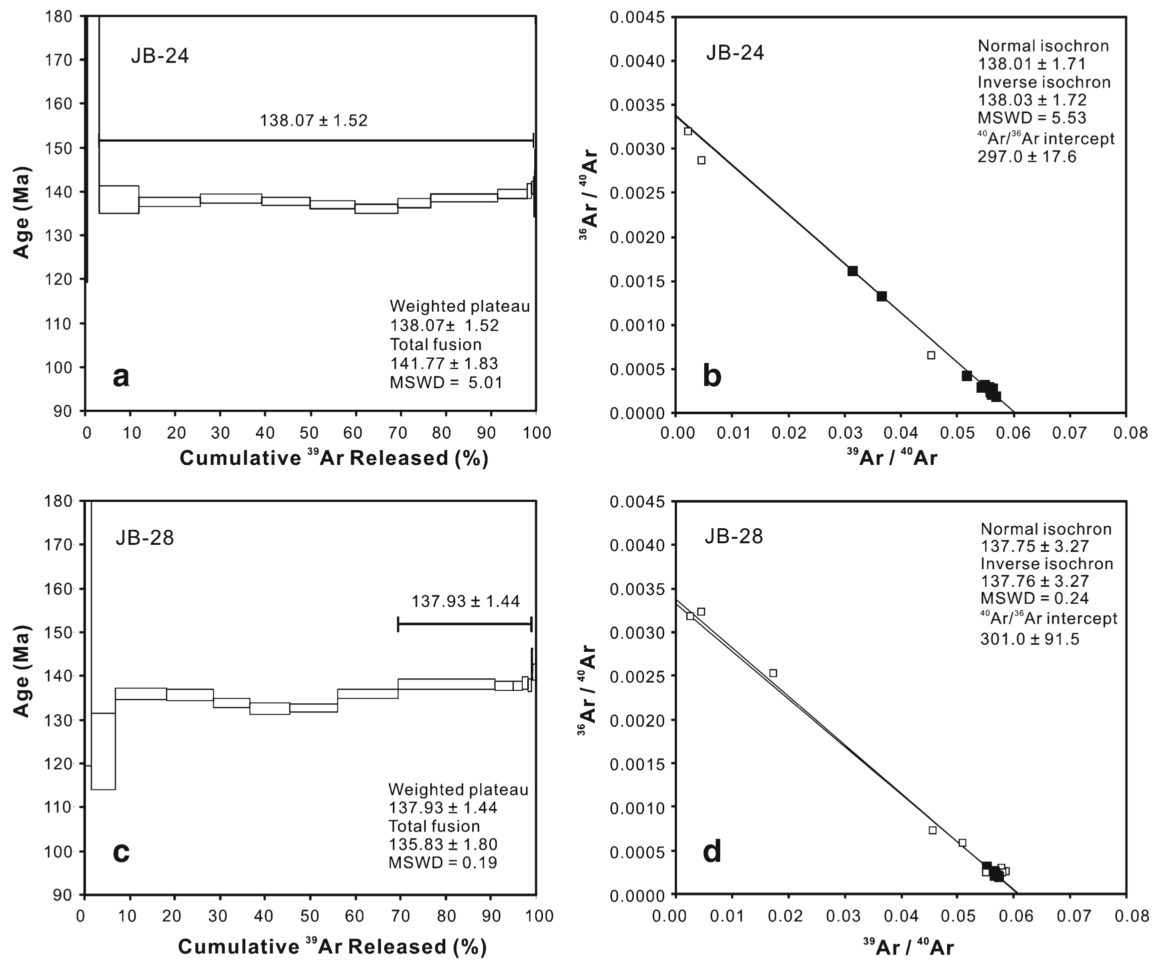

Fig. 5 ^{40}Ar/^{39}Ar age spectrum and inverse isochrons for two muscovite samples from the Jubankeng tungsten deposit, Northern Guangdong. The *solid squares* represent the steps selected for inverse isochron age calculation

Muscovite ^{40}Ar/^{39}Ar plateau age represents an alteration event that is associated to tungsten mineralization, and therefore the ^{40}Ar/^{39}Ar plateau age of muscovite sample JB-24 (138.1± 1.5 Ma) is interpreted here as the mineralization age of Jubankeng tungsten deposit. This age is similar to previously reported muscovite and lepidolite K-Ar ages of 134 and 140 Ma, respectively (RGNTD 1985), and consistent with an ^{40}Ar/^{39}Ar age of ~140 Ma for the regional mafic dikes from the Zhuguangshan and Guidong batholith (Li et al. 1997), as well as with a Rb–Sr isochron age of 136–137 Ma for the second stage granite from Qianlishan, Southern Hunan (Mao et al. 1995) and a zircon SHRIMP U-Pb age (137±2 Ma) for the Ejinao A-type granite from Middle Guangdong (Wang et al. 2005). The data indicates that this event corresponds to a second episode of tungsten mineralization in Northern Guangdong.

Metallogenic epochs of W–Sn mineralization in Nanling region

Peng et al. (2007, 2008) regarded large-scale W–Sn mineralization in Nanling Region as occurring mainly at 150–160 Ma, while Mao et al. (2007) emphasized that mineralization occurred within two stages: (1) Late Jurassic–Early Cretaceous (165–150 Ma), and (2) middle Cretaceous (130–90 Ma). In the past few years, more geochronological ages for the tungsten–tin polymetallic deposits in the Nanling region have been determined by several researchers using ^{40}Ar/^{39}Ar and Re–Os isotopic dating methods. A summary of available information on 31 W–Sn–(Pb–Zn) polymetallic deposits is shown in Table 3. When all 54 ages of these deposits are statistically analyzed, three main age clusters can be identified: an oldest group at 210–235 Ma, which includes four deposits, a second and most important cluster at 130–165 Ma that involves 24 deposits, and a third group at 90–100 Ma, which includes three deposits (Table 3). The second age cluster can be further divided into two episodes, 134–140 and 144–162 Ma (most dates range from 150 to 160 Ma) with a maximum frequency at 154–156 Ma. Therefore, large-scale W-Sn mineralization in Nanling region mainly occurred at 150–160 Ma (Mao et al. 2007; Peng et al. 2007, 2008). The extension-induced deep crustal melting and underplating of mantle-derived basaltic melts are suggested as the two main driving mechanisms for

Table 3 Summary of geochronological data for W-Sn polymetallic deposits in South China

Deposit name	Igneous rock types/ages	Host rocks	Metals	Reserve (Mt)/Grade (%)	Geological characteristics	Deposit type	Mineral dated/method	Age ± 2σ (Ma)	Reference
Southern Hunan									
Shizhuyuan	Qianlishan granite	Devonian limestones	W–Sn–Mo–Bi–F–Pb–Zn	WO_3: 70.13 Grade: 0.344	Ore-bodies occur near the contact zone between granite and limestone	Skarn and greisen	mo/Re–Os	151.0±3.5	Li et al. (1996)
						Skarn and greisen	ms/^{40}Ar/^{39}Ar	153.4±0.2	Mao et al. (2004)
						Skarn and greisen	ms/^{40}Ar/^{39}Ar	134.0±1.6	Mao et al. (2004)
Furong	Qitianling granite, 156–162 Ma	Permian—carboniferous limestones with intercalated siltstones	Sn	Sn: >60 Grade: 0.3–1.5	Tin mineralization styles include altered granite-type, tectonic al teration zone-type, skarn-, porphyry-, greisen-, and quartz vein-type mineralization. Ore-bodies occur within stock and outer contact zone	Greisen	ms/^{40}Ar-^{39}Ar	156.1±0.4	Mao et al. (2004)
						Greisen	ms/^{40}Ar-^{39}Ar	160.1±0.9	Mao et al. (2004)
						Quartz vein	phl/^{40}Ar-^{39}Ar	150.6±1.0	Peng et al. (2007)
						Quartz vein	phl/^{40}Ar-^{39}Ar	154.7±1.1	Peng et al. (2007)
						Quartz vein	phl/^{40}Ar-^{39}Ar	157.3±1.0	Peng et al. (2007)
						Quartz vein	amph/^{40}Ar-^{39}Ar	156.9±1.1	Peng et al. (2007)
						Quartz vein	ms/^{40}Ar-^{39}Ar	159.9±0.5	Peng et al. (2007)
						Quartz vein	ms/^{40}Ar-^{39}Ar	154.8±0.6	Peng et al. (2007)
Xintianling	Qitianling granite, 156–162 Ma	Carboniferous limestones with intercalated siltstones	W–Mo–Bi–Cu–Pb–Zn	WO_3: 30.31 Grade: 0.37	Skarn-type scheelite ore-bodies occur within the contact zone between northern part of Qitianling pluton and limestones	Skarn	Annite/^{40}Ar-^{39}Ar	157.1±0.3	Mao et al. (2004)
Huangshaping	Dacite- porphyry and quartz-porphyry, 161.6±1.1 Ma	Lower Carboniferous dolomites, sandstones	Pb–Zn–W–Mo	WO_3: 9.10 Grade: 0.254	Ore-bodies occur within the inner- and outer-contact zones of the Huangshaping granite porphyry, hosted mainly by skarn and porphyry	Skarn	mo/Re–Os	153.8±4.8	Ma et al. (2007)
						Skarn	mo/Re–Os	154.8±1.9	Yao et al. (2007)
Xianghualing	Granite- porphyry and quartz- porphyry	Devonian limestones, sandstones and Carboniferous limestones and clastic rocks	Sn–W–Pb–Zn	Sn: 4.52 Grade: 0.02–3.97	Ore mineralization consists of mainly granite-type, skarn-type, and hydrothermal filling type mineralization	Greisen	ms/^{40}Ar-^{39}Ar	161.3±1.1	Yuan et al. (2007)
						Greisen	ms/^{40}Ar-^{39}Ar	154.4±1.1	Yuan et al. (2007)
						Greisen	ms/^{40}Ar-^{39}Ar	158.7±1.2	Yuan et al. (2007)
Hehuaping	Wangxianling granite, 212±4 Ma	Devonian limestones and sandstones	Sn–Bi–Pb–Zn	Sn: 8.5 Grade: 0.28–1.82	Ore-bodies consist of mainly Sn-bearing skarn and cassiterite-sulfides	Skarn	mo/Re–Os	224.0±1.9	Cai et al. (2006)
Da'ao and Guagouchong	Granite, 151~156 Ma	Sinian-Cambrian metamorphosed sandstones and slates	W–Sn	WO_3: 5.16 Grade: 0.15–0.66 Sn: 3.39 Grade: 0.02–1.02	Tungsten mineralization includes mainly greisen-type, and a few fracture zones altered rock-type, altered granite-type, greisen-type, and quartz vein-type mineralization	Greisen/quartz vein	mo/Re–Os	151.3±2.4	Fu et al. (2007)
Yaogangxian	Yaogangxian granite	Cambrian metasandstones and slates, unconformably	W	WO_3: 26.64 Grade: 0.29–1.269	Ore mineralization consists of mainly quartz vein-type	Quartz vein	mo/Re-Os	154.9±2.6	Peng et al. (2006)

Table 3 (continued)

Deposit name	Igneous rock types/ages	Host rocks	Metals	Reserve (Mt)/Grade (%)	Geological characteristics	Deposit type	Mineral dated/method	Age ± 2σ (Ma)	Reference
		overlain by Devonian and Carboniferous sandstones and limestones, and Jurassic sandstones			wolframite and skarn-type scheelite mineralization. Most ore veins occur along the northern contact zone between the granite and the sedimentary strata and commonly crosscut both lithological rocks	Quartz vein	phl/^{40}Ar-^{39}Ar	153.0±1.1	Peng et al. (2006)
						Quartz vein	ms/^{40}Ar-^{39}Ar	155.1±1.1	Peng et al. (2006)
Longshang Mine, Xitian	Xitian granite, 151–165 Ma	Devonian limestones	Sn-W	Sn: 5.86 Grade: 0.524 WO_3: 4.63 Grade: 0.566	Ore-bodies occur within the contact zone, and the mineralization consists of mainly skarn-type and fracture zone-altered rock type mineralization	skarn	ms/^{40}Ar-^{39}Ar	155.6±1.3	Ma et al. (2008)
						Greisen	ms/^{40}Ar-^{39}Ar	157.2±1.4	Ma et al. (2008)
Jiebeiling	Granite- porphyry	Carboniferous limestones	Sn-Be	Sn: 7.6 Grade: 0.8	Ore-bodies occur within the contact zone between granite-porphyry, cryptoexplosive breccia and limestones	Greisen-porphyry	bio/^{40}Ar-^{39}Ar	91.1±1.1	Mao et al. (2007)
Southern Jiangxi									
Dajishan	Concealed granite, 151.7±1.6 Ma	Cambrian metamorphosed sandstones and slates	W-Bi	WO_3: 15.34 Grade: 1.904	Quartz-wolframite veins distributed in the outer contact zone between granite and sandstone	Quartz vein	ms/^{40}Ar-^{39}Ar	144.4±0.5	Zhang et al. (2006)
						Quartz vein	ms/^{40}Ar-^{39}Ar	147.2±0.6	Zhang et al. (2006)
Muziyuan	Granite, 153.3±1.9 Ma	Cambrian metamorphosed sandstones and slates	W	WO_3: 0.55 Grade:0.958	Ore-bodies consist of quartz–wolframite thick veins and veinlets	Quartz vein	mo/Re–Os	155.0±2.4	Zhang et al. (2009)
Taoxikeng	Concealed granite	Sinian-Cambrian and Ordovician metamorphosed sandstones and slates	W	WO_3: 1.22 Grade: 0.987	Quartz–wolframite veins distributed in the outer contact zone	Quartz vein	mo/Re–Os	154.4±3.8	Chen et al. (2006)
						Quartz vein	ms/^{40}Ar-^{39}Ar	152.7±1.5	Guo et al. (2008)
						Quartz vein	ms/^{40}Ar-^{39}Ar	153.4±1.3	Guo et al. (2008)
						Quartz vein	ms/^{40}Ar-^{39}Ar	155.0±1.4	Guo et al. (2008)
Piaotang	Concealed granite	Cambrian metamorphosed sandstones and slates	W–Sn–Cu–Pb–Zn	WO_3: 8.94 Grade: 0.203	Ore-bodies consist of the quartz–wolframite thick veins and veinlets	Quartz vein	ms/^{40}Ar-^{39}Ar	153.6±1.5	Chen et al. (2006)
						Quartz vein	ms/^{40}Ar-^{39}Ar	158.9±1.4	Liu et al. (2008a, b)
						Quartz vein	ms/^{40}Ar-^{39}Ar	152.0±1.9	Zhang et al. (2009)
Keshuling	Granite	Cambrian-Ordovician metamorphosed sandstones and slates	W–Sn	WO_3: <1.0	Quartz-wolframite veins distributed in Ordovician sandstone	Quartz vein	ms/^{40}Ar–^{39}Ar	158.8±1.2	Liu et al. (2008a, b)
Maoping	Granite	Cambrian metamorphosed sandstones and slates	W–Sn	WO_3: 10.88 Grade: 0.13	Ore-bodies consist of upper quartz–wolframite thick veins and lower greisen-type ore	Greisen	mo/Re–Os	156.8±3.9	Zeng et al. (2009)
Niuling	Concealed granite	Cambrian metamorphosed sandstones and slates	W–Sn	WO_3: 3.0	Quartz-wolframite veins distributed within inner contact zone	Quartz vein	mo/Re–Os	154.9±4.1	Feng et al. (2007b)
Yaolanzhai	Granite, 156.9±1.7 Ma	Cambrian metamorphosed sandstones and slates	W	WO_3: <1.0	Ore-bodies consist of altered granite	Altered granite	mo/Re-Os	155.8±2.8	Feng et al. (2007a)

Table 3 (continued)

Deposit name	Igneous rock types/ages	Host rocks	Metals	Reserve (Mt)/Grade (%)	Geological characteristics	Deposit type	Mineral dated/method	Age ± 2σ (Ma)	Reference
Xian'etang		Sinian metamorphosed sandstones and slates	Sn–W	WO_3: <1.0	Quartz–wolframite veins distributed in Sinian sandstones	Quartz vein	ms/^{40}Ar–^{39}Ar	231.4±2.4	Liu et al. (2008a, b)
Northern Guangdong									
Shirenzhang	Granite	Cambrian-Ordovician metamorphosed sandstones and slates	W	WO_3: 2.17 Grade: 0.52	Quartz-wolframite veins distributed in the inner and outer contact zone between granite and sandstone	Quartz vein	mo/Re–Os	159.1±2.2	Fu et al. (2008)
Shigushan	Granite	Cambrian metamorphosed sandstones and slates	W–Bi	WO_3: 0.65	Ore-bodies consist of the quartz–wolframite thick veins and veinlets	quartz vein	mo/Re-Os	154.2±2.7	Fu et al. (2008)
Hongling	Granite	Granites	W	WO_3: >3 Grade: 0.13	Ore-bodies consist of the upper quartz–wolframite veins and lower altered granite-type scheelite ore	Quartz vein/altered granite	mo/Re–Os	159.1±1.5	Wang et al. (2010)
Meiziwo	Caledonian granodiorite	Cambrian-Ordovician metamorphosed sandstones and slates	W	WO_3: 2.38 Grade: 0.799	Tungsten-containing quartz veins controlled by the NW-trending fractures	Quartz vein Quartz vein	mo/Re–Os ms/^{40}Ar–^{39}Ar	157.7±1.4 155.97±0.59	This paper Zhai et al. (2010)
Yaoling	Granite	Cambrian- Devonian low-grade meta-sedime-ntary quartzites, slates and limestones	W	WO_3: 3.63 Grade: 1.29	Involves quartz-wolframite vein-type, skarn-type and altered granite-type scheelite mineralization	Quartz vein	mo/Re–Os	159.5±2.8	This paper
Jubankeng		Cambrian metamorphosed sandstones and slates	W–Sn–Zn–Cu	WO_3: 10.03 Grade: 0.63	Quartz–wolframite veins distributed in the strata	Quartz vein Quartz vein	ms/^{40}Ar-^{39}Ar ms/^{40}Ar-^{39}Ar	138.07±1.72 139.2±1.5	This paper Fu et al. (2009)
Other deposits									
Xingluokeng, Fujian	Granitic porphyry, 155–157 Ma	Sinian-Cambrian and Devonian quartz sandstones, siltstones	W–Mo	WO_3: 30.43 Grade: 0.233	Disseminated scheelite and a few W-Mo quartz veins distribute within porphyry.	Altered porphyry	mo/Re–Os	156.3±4.8	Zhang et al. (2008)
Hukeng, Jiangxi	Granite	Sinian schists, gneisses, migmatites	W	WO_3: 5.94 Grade: 1.525	Quartz-wolframite veins distributed in granite	Quartz vein	mo/Re–Os	150.2±2.2	Liu et al. (2008a, b)
Damingshan, Guangxi	Porphyritic muscovite granite	Cambrian quartz sandstones and lower Devonian sandstones	W	WO_3: 16.02 Grade: 0.236	Quartz veins distribute within strata and granite, Disseminated scheelite distribute within altered granite	Quartz vein- and altered granite	mo/Re–Os	95.40±0.97	Li et al. (2008)
Wangshe, Guangxi	Late Jurassic biotite granite	Granites	Cu–W–Mo–Bi	Grade: 0.11	Quartz veins distribute along NW and NE striking	Quartz vein	mo/Re–Os	93.8±4.6	Lin et al. (2008)
Liguifu, Northeastern Guangxi	Granite, 209 Ma	Granites	W–Sn–Mo	WO_3: 1.14 Grade: 0.557	Ore bodies occur within N-S strike secondary cracks	Mainly greisen-/quartz vein	mo/Re–Os	211.9±6.4	Zou et al. (2009)
Limu, Northeastern Guangxi	Granite	Upper Devonian and lower Carboniferous limestones	Nb–Ta–W–Sn	WO_3: 1.11 Sn: 0.79	From top to bottom, the deposit consists of quartz-vein type W ore-bodies, granitic pegmatite type tantalum and niobium ore-bodies, and granite-type tantalum, niobium and tin ore-bodies	Greisen-/pegmatite-/altered granite	ms/^{40}Ar–^{39}Ar	214.1±1.9	Yang et al. (2009)

Reserves data from http://www.chinamining.com.cn/report/default.asp?V_DOC_ID=1123, ECDMDCVJX (1996), ECDMDCVGD (1996), ECDMDCVGX (1996), Huang et al. (2001), Wu (2006), http://www.hunangtzy.com/web/mine_zhuanlan_detail.jsp?docid=33824 and http://www.hn409.com/newsview.asp?id=885

amph amphibole, *bio* biotite, *mo* molybdenite, *ms* muscovite, *phl* phlogopite the Late Jurassic granitic magmatism in South China (Zhou et al. 2006). The simultaneity of the Late Jurassic large-scale granitic magmatism and large-scale W–Sn mineralization in the Nanling region (Mao et al. 2007; Peng et al. 2008) suggests that large-scale W–Sn mineralization is related to the same extensional processes.

Conclusions

Two episodes of Late Jurassic W–Sn polymetallic mineralization are recognized in Northern Guangdong. An early episode of tungsten mineralization represented by the Yaoling, Hongling and Meiziwo deposits, during the Late Jurassic (158–159 Ma), and a younger episode represented by the Jubankeng tungsten deposit during the Early Cretaceous (~138 Ma). W–Sn mineralization in the Nanling region occurred in several intervals at 90–100, 134–140, 144–162, and 210–235 Ma. The most important large-scale W–Sn mineralization event occurred within a 10 Ma timeframe during the Late Jurassic (150–160 Ma).

Acknowledgments National Basic Research Program of China (2007CB411408) financially supported this research. We would like to thank Meiziwo, Yaoling, and Jubankeng tungsten mines and chief engineer Ba Zhu of the 290 Institute of Nuclear Industry for their support during field geological survey and sampling, Guangdong Metallurgical and Geological Team 932 for providing exploration reports of regional tungsten deposits. The useful suggestions and comments of Fernando Barra (Associate editor) and an anonymous reviewer improved the English and quality of this manuscript.

References

Cai MH, Chen KX, Qu WJ, Liu GQ, Fu JM, Yin JP (2006) Geological characteristics and Re–Os dating of molybdenites in Hehuaping tin-polymetallic deposit, Southern Hunan Province. Miner Deposits 25:263–268 (in Chinese with English abstract)

Chen GL (1983) Types and characteristics of tungsten ore deposits in northern Guangdong, China (in Chinese with English abstract). Acta Geologica Sinica 142–153

Chen ZH, Wang DH, Qu WJ, Chen YC, Wang PA, Xu JX, Zhang JJ, Xu ML (2006) Geological characteristics and mineralization age of the Taoxikeng tungsten deposit in Chongyi County, southern Jiangxi Province, China. Geol Bull China 25:496–501 (in Chinese with English abstract)

Creaser R, Sannigarhi P, Chacko T, Selby D (2002) Further evaluation of the Re–Os geochronometer in organic-rich sedimentary rocks: a test of hydrothermal maturation effects in the Exshaw Formation, Western Canada sedimentary basin. Geochim Cosmochim Acta 66:3441–3452

Du AD, Wu SQ, Sun DZ, Wang SX, Qu WJ, Markey RJ, Stein HJ, Morgan JW, Malinovskiy D (2004) Preparation and certification of Re–Os dating reference materials: molybdenite HLP and JDC. Geostand Geoanalytical Res 28:41–52

Du AD, Qu WJ, Wang DH, Li HM, Feng CY, Liu H, Ren J, Zeng FG (2007) Subgrain-size decoupling of Re and ^{187}Os within molybdenite. Miner Deposits 26:572–580 (in Chinese with English abstract)

Editorial Committee of the discovery of mineral deposits of China - Volume of Guangdong Province (ECDMDCVGD) (1996) The discovery of mineral deposits of China—volume of Guangdong Province (in Chinese with English abstract). Geological Publishing House, Beijing, pp 116–136

Editorial Committee of the discovery of mineral deposits of China - Volume of Guangxi Zhuang Autonomous Region (ECDMDCVGX) (1996) The discovery of mineral deposits of China—volume of Guangxi Zhuang Autonomous Region (in Chinese with English abstract). Geological Publishing House, Beijing, pp 116–136

Editorial Committee of the discovery of mineral deposits of China -Volume of Jiangxi Province (ECDMDCVJX) (1996) The discovery of mineral deposits of China—volume of Jiangxi Province (in Chinese with English abstract). Geological Publishing House, Beijing, pp 80–112

Feng CY, Feng YD, Xu JX, Zeng ZL, She HQ, Zhang DQ, Qu WJ, Du AD (2007a) Isotope chronological evidence for Upper Jurassic petrogenesis and mineralization of altered granite-type tungsten deposits in the Zhangtiantang area, Southern Jiangxi. Geol China 34:642–650 (in Chinese with English abstract)

Feng CY, Xu JX, Zeng ZL, Zhang DQ, Qu WJ, She HQ, Li JW, Li DX, Du AD, Dong YJ (2007b) Zircon SHRIMP U-Pb and molybdenite Re–Os dating in Tianmenshan–Hongtaoling tungsten–tin Orefield, Southern Jiangxi Province, China, and its geological implication. Acta Geol Sin 81:952–963 (in Chinese with English abstract)

Fraser GL, Hussey K, Compstond DM (2008) Timing of Palaeoproterozoic Au-Cu-Bi and W-mineralization in the Tennant Creek region, northern Australia: Improved constraints via intercalibration of ^{40}Ar/^{39}Ar and U-Pb ages. Precambrian Res 164:50–65

Fu JM, Li HQ, Qu WJ, Yang XJ, Wei JQ, Liu GQ, Ma LY (2007) Re-Os isotope dating of the Da'ao tungsten-tin deposit in the Jiuyi Mountains, southern Hunan Province. Geol China 34:651–656 (in Chinese with English abstract)

Fu JM, Li HQ, Qu WJ, Ma LY, Yang XQ, Wei JQ, Liu GQ (2008) Determination of mineralization epoch of quartz-vein type tungsten deposits in Shixing region, Northern Guangdong and its geological significance. Geotecton Metallog 32:57–62 (in Chinese with English abstract)

Fu JM, Li XN, Cheng SB, Xu DR, Ma LY, Chen XQ (2009) Metallogenic ages of tungsten–tin polymetallic deposits in Lianping area, northern Guangdong Province. Geol China 36:1331–1339 (in Chinese with English abstract)

Guangdong Metallurgical and Geological Team 932 (1966) How do we use "five-story building" model to search, evaluate and prospect wolframite-quartz vein deposits. Geol Explor 5:15–19 (in Chinese)

Guangdong Metallurgical and Geological Team 932 (1967) Adhere to "practice" and understanding of "five-story building" metallogenic regularity of vein tungsten deposits. Geol Explor 3:11–16 (in Chinese)

Guangdong Metallurgical and Geological Team 932 (1976) Summary report on the exploration of the Shirenzhang tungsten deposit, Guangdong Province (in Chinese). Internal report pp 1–25

Guo CL, Lin ZY, Wang DH, Chen W, Zhang Y, Feng CY, Chen ZH, Zeng ZL, Cai RQ (2008) Petrologic characteristics of the granites and greisens and muscovite ^{40}Ar/^{39}Ar dating in the Taoxikeng tungsten polymetallic deposit, Southern Jiangxi province. Acta Geol Sin 82:1274–1284

Hall CM, Walter RC, Westgater JA, York D (1984) Geochronology, stratigraphy and geochemistry of Cindery Tuff in Pliocene hominid-bearing sediments of the Middle Awash, Ethiopia. Nature 308:26–31

Huang GF, Zemg QW, Wei SL, Xu YM, Hou MS, Kang WQ (2001) Geological characteristics and ore-controlling factors of the Furong orefield, Qitianling, Hunan. Chinese Geol 28:30–34 (in Chinese with English abstract)

Koppers AAP (2002) ArArCALC-software for $^{40}Ar/^{39}Ar$ age calculations. Comput Geosci 28:605–619

Lee JY, Marti K, Severinghaus JP, Kawamura K, Yoo HS, Lee JB, Kim JS (2006) A redetermination of the isotopic abundances of atmospheric Ar. Geochim Cosmochim Acta 70:4507–4512

Li HY, Mao JW, Sun YL, Zou XQ, He HL, Du AD (1996) Re–Os isotopic chronometry of molybdenite in the Shizhuyuan polymetallic tungsten deposit, Southern Hunan. Geol Rev 42:261–267 (in Chinese with English abstract)

Li JW, Li XH, Pei RF, Mei YX, Wang YL, Qu WJ, Huang XB, Zhang WS (2007) Re-Os age of molybdenite from the southern ore zone of the Wushan copper deposit, Jiangxi Province, and its geological significance. Acta Geol Sin 81:801–807 (in Chinese with English abstract)

Li SR, Wang DH, Liang T, Qu WJ, Ying LJ (2008) Metallogenic epochs of the Damingshan tungsten deposit in Guangxi and its prospecting potential. Acta Geol Sin 82:873–879 (in Chinese with English abstract)

Li XH, Hu RZ, Rao B (1997) Geochronology and geochemistry of cretaceous mafic dikes from Northern Guangdong, SE China. Geochimica 26:14–31 (in Chinese with English abstract)

Lin ZY, Wang DH, Li SR (2008) Re-Os isotopic age of molybdenite from the Wangshe copper–tungsten deposit in Guangxi province and their implications. Acta Geol Sin 82:1565–1571 (in Chinese with English abstract)

Liu YJ, Ma DS (1993) Vein-type tungsten deposits of China and adjoining regions. Ore Geol Rev 8:233–246

Liu J, Ye HS, Xie GQ, Yang GQ, Zhang W (2008a) Re-Os dating of molybdenite from the Hukeng tungsten deposit in the Wugongshan area, Jiangxi Province, and its geological implications. Acta Geol Sin 82:1572–1579 (in Chinese with English abstract)

Liu SB, Wang DH, Chen YC, Li JK, Ying LJ, Xu JX, Zeng ZL (2008b) $^{40}Ar/^{39}Ar$ ages of muscovite from different types tungsten-bearing quartz veins in the Chong-Yu-You concentrated mineral area in Gannan region and its geological significance. Acta Geol Sin 82:932–940

Lu YF, Ma LY, Qu WJ, Mei YP, Chen XQ (2006) U-Pb and Re-Os isotope geochronology of Baoshan Cu–Mo polymetallic ore deposit in Hunan province. Acta Petrol Sin 22:2483–2492 (in Chinese with English abstract)

Luck JM, Allègre CJ (1982) The study of molybdenites through the ^{187}Re-^{187}Os chronometer. Earth Planet Sci Lett 61:291–296

Ludwig KR (2004) Isoplot/Ex, version 3.0: a geochronological tool kit for Microsoft Excel. Berkeley Geochronology Center, Berkeley

Luo HM, Xiao GM, Tang K (2006) Characteristics of tungsten poly-metal metallogenic belt and ore prospecting orientation in Chengkou–Jiulian area, Northern Guangdong Province. Resour Survey Environ 27:127–135 (in Chinese with English abstract)

Ma LY, Fu JM, Wu SC, Xu DM, Yang XJ (2008) $^{40}Ar/^{39}Ar$ isotopic dating of the Longshang tin-polymetallic deposit, Xitian orefield, eastern Hunan. Geology In China 35:706–713 (in Chinese with English abstract)

Ma LY, Lu YF, Qu WJ, Fu JM (2007) Re–Os isotopic chronology of molybdenites in Huangshaping lead–zinc deposit, southeast Hunan, and its geological implications. Miner Deposits 26:425–431 (in Chinese with English abstract)

Mao JW, Li HY, Pei RF (1995) Nd-Sr isotopic and petrogenetic studies of the Qianlishan granite stock, Hunan province. Miner Deposits 14:235–242 (in Chinese with English abstract)

Mao JW, Xie GQ, Li XF, Zhang CQ, Mei YX (2004) Mesozoic large scale mineralization and multiple lithospheric extension in South China. Earth Sci Front 11:45–55 (in Chinese with English abstract)

Mao JW, Xie GQ, Guo CL, Chen YC (2007) Large–scale tungsten-tin mineralization in the Nanling region, South China: Metallogenic ages and corresponding geodynamic processes. Acta Petrol Sin 23:2329–2338 (in Chinese with English abstract)

Mao JW, Xie GQ, Bierlein F, Qu WJ, Du AD, Ye HS, Pirajno F, Li HM, Guo BJ, Li YF, Yang ZQ (2009) Tectonic implications from Re–Os dating of Mesozoic molybdenum deposits in the East Qinling–Dabie orogenic belt. Geochim Cosmochim Acta 72:4607–4626

Nier AO (1937) The isotopic constitution of osmium. Phys Rev 52:885–892

Nier AO (1950) A redetermination of the relative abundances of the isotopes of carbon, nitrogen, oxygen, argon, and potassium. Phys Rev 77:789–793

Peng JT, Zhou MF, Hu RZ, Shen NP, Yuan SD, Bi XW, Du AD, Qu WJ (2006) Precise molybdenite Re–Os and mica Ar–Ar dating of the Mesozoic Yaogangxian tungsten deposit, central Nanling district, South China. Miner Deposita 41:661–669

Peng JT, Hu RZ, Bi XW, Dai TM, Li ZL, Li XM, Shuang Y, Yuan SD, Liu SR (2007) $^{40}Ar/^{39}Ar$ isotopic dating of tin mineralization in Furong deposit of Hunan province and its geological significance. Miner Deposits 26:237–248 (in Chinese with English abstract)

Peng JT, Hu RZ, Yuan SD, Bi XW, Shen NP (2008) The time ranges of granitoid emplacement and related nonferrous metallic mineralization in southern Hunan. Geol Rev 54:617–625 (in Chinese with English abstract)

Reynolds P, Ravenhurst C, Zentilli M, Lindsay D (1998) High-precision ^{40}Ar-^{39}Ar dating of two consecutive hydrothermal events in the Chuquicamata porphyry copper system, Chile. Chem Geol 148:45–60

RGNTD (Research Group for Nanling Tungsten Deposits, Chinese Ministry of Metallurgy) (1985) Tungsten deposits in South China (in Chinese with English abstract). Publishing House of Metallurgical Industry, Beijing, pp 1–496

Selby D, Creaser RA (2001) Re-Os geochronology and systematics in molybdenite from the Endako porphyry molybdenum deposit, British Columbia, Canada. Econ Geol 96:197–204

Selby D, Creaser RA (2004) Macroscale NTIMS and microscale LA-MC-ICP-MS Re–Os isotopic analysis of molybdenite: testing spatial restrictions for reliable Re–Os age determinations, and implications for the decoupling of Re and Os within molybdenite. Geochim Cosmochim Acta 68:3897–3908

Smoliar MI, Walker RJ, Morgan JW (1996) Re–Os ages of group IIA, IIIB, IVA, IVB iron meteorites. Science 271:1099–1102

Steiger RH, Jäger E (1977) Subcommision on Geochronology: Convention on the use of decay constants in geo- and cosmochronology. Earth Planet Sci Lett 36(359):362

Stein HJ, Scherstén A, Hannah JL, Markey RJ (2003) Subgrain-scale decoupling of Re and ^{187}Os and assessment of laser ablation ICP-MS spot dating in molybdenite. Geochim Cosmochim Acta 67:3673–3686

Suzuki K, Shimizu H, Masuda A (1996) Re-Os dating of molybdenites from ore deposits in Japan: implication for the closure temperature of the Re-Os system for molybdenite and the cooling history of molybdenum ore deposits. Geochim Cosmochim Acta 60:3151–3159

Takahashi Y, Uruga T, Suzuki K, Tanida H, Terada Y, Hattori KH (2007) An atomic level study of rhenium and radiogenic osmium in molybdenite. Geochim Cosmochim Acta 71:5180–5190

Wang Q, Zhao ZH, Jian P, Xiong XL, Bao ZW, Dai TM, Xu JF, Ma JL (2005) Geochronology of Cretaceous A-type granitoids or alkaline intrusive rocks in the hinterland, South China: Constraints for late-Mesozoic tectonic evolution. Acta Petrol Sinica 21:795–808 (in Chinese with English abstract)

Wang Y, Chen MX, Li MG, Zeng YX (2006) Study on variety and rule of mineralization in Yaoling tunsten mine in Guangdong province, South China. Miner Res Geol 20:334–339 (in Chinese with English abstract)

Wang YL, Pei RF, Li JW, Qu WJ, Li L, Wang HL, Du AD (2008a) Re–Os dating of molybdenite from the Yaogangxian Tungsten

Deposit, South China, and its geological significance. Acta Geol Sin 82:820–825 (in Chinese with English abstract)
Wang ZL, Yang ZM, Yang ZS, Tian SH, Liu YC, Ma YQ, Wang GR, Qu WJ (2008b) Narigongma porphyry molybdenite copper deposit, northern extension of Yulong copper belt: evidence from the age of Re–Os isotope. Acta Petrol Sin 24:503–510
Wang XF, Qi HW, Hu RZ, Qu WJ, Peng JT, Bi XW (2010) Re–Os isotopic chronology of molybdenites from Hongling tungsten deposit of Guangdong province and its geological significance. Miner Deposits 29:415–427 (in Chinese with English abstract)
Wu SN (2006) Geological characteristics of the Hehuaping tin polymetallic deposit in Chenzhou, Hunan province. Miner Res Geol 20:43–46 (in Chinese with English abstract)
Xie GQ, Zhao HJ, Zhao CS, Li XQ, Hou KJ, Pan HJ (2009) Re-Os dating of molybdenite from Tongliishan ore district in southeastern Hubei Province, Middle–Lower Yangtze River belt and its geological significance. Miner Deposits 28:227–239 (in Chinese with English abstract)
Yang F, Li XF, Feng ZH, Bai YP (2009) $^{40}Ar/^{39}Ar$ dating of muscovite from greisenized granite and geological significance in Limu tin deposit. J Guilin Univ Technol 29:21–24 (in Chinese with English abstract)
Yao JM, Hua RM, Qu WJ, Qi HW, Lin JF, Du AD (2007) Re-Os isotope dating of molybdenites in the Huangshaping Pb-Zn-W-Mo polymetallic deposit, Hunan province, South China and its geological significance. Sci China Series D: Earth Sci 50:519–526
Yuan SD, Peng JT, Shen NP, Hu RZ, Dai TM (2007) ^{40}Ar-^{39}Ar isotopic dating of the Xianghualing Sn-polymetallic orefield in southern Hunan and its geological implications. Acta Geol Sin 81:278–286 (in Chinese with English abstract)
Zeng ZL, Zhang YZ, Zhu XP, Chen ZH, Wang CH, Qu WJ (2009) Re-Os isotopic dating of molybdenite from the Maopjng tungsten-tin deposit in Chongyi county of Southern Jiangxi province and its geological significance. Rock Miner Anal 28:209–214 (in Chinese with English abstract)
Zhai W, Sun XM, Wu YS, Sun HY, Hua RM, Yang YQ, Li WQ, Li SH (2010) Zircon SHRIMP U-Pb dating of the buried granodiorite and muscovite $^{40}Ar/^{39}Ar$ dating of mineralization and geological implications of Meiziwo tungsten deposit, northern Guangdong province, China. Geol J China Univ 16:177–185 (in Chinese with English abstract)
Zhang WL, Hua RM, Wang RC, Chen PR, Li HM (2006) New dating of the Dajishan granite and related tungsten mineralization in Southern Jiangxi. Acta Geol Sin 80:956–962 (in Chinese with English abstract)
Zhang JX, Chen ZH, Wang DH, Chen ZY, Liu SB, Wang CH (2008) Geological characteristics and metallogenic epoch of the Xingluokeng tungsten deposit, Fujian province. Geotecton Metallog 32:92–97 (in Chinese with English abstract)
Zhang WL, Hua RM, Wang RC, Li HM, Qu WJ, Ji JQ (2009) New dating of the Piaotang granite and related tungsten mineralization in Southern Jiangxi. Acta Geol Sin 83:659–670 (in Chinese with English abstract)
Zhou XM, Sun T, Shen WZ, Shu LS, Niu YL (2006) Petrogenesis of Mesozoic granitoids and volcanic rocks in South China: a response to tectonic evolution. Episodes 29:26–33
Zou XW, Cui S, Qu WJ, Bai YS, Chen XQ (2009) Re-Os isotope dating of the Liguifu tungsten–tin polymetallic deposit in Dupangling area, Guangxi. Geol China 36:837–844 (in Chinese with English abstract)